The alignment of cylindrically layered smectic A liquid crystals with director tilt on the boundaries

2008 J. Phys. A: Math. Theor. 41 385205

(http://iopscience.iop.org/1751-8121/41/38/385205)

IOP PUBLISHING JOURNAL OF PHYSICS A: MATHEMATICAL AND THEORETICAL

J. Phys. A: Math. Theor. **41** (2008) 385205 (20pp) doi:10.1088/1751-8113/41/38/385205

The alignment of cylindrically layered smectic A liquid crystals with director tilt on the boundaries

A J Walker

Department of Mathematics, University of Strathclyde, Livingstone Tower, 26 Richmond Street, Glasgow, G1 1XH, UK

E-mail: ta.awal@maths.strath.ac.uk

Received 10 April 2008, in final form 25 July 2008
Published 26 August 2008
Online at stacks.iop.org/JPhysA/41/385205

Abstract

A novel method for constructing a nonlinear smectic layer function is outlined and employed to construct free energy density functions for two theoretical experiments involving cylindrically layered smectic A liquid crystals. Director tilt on the boundaries is imposed and it is assumed that the layer normal **a** and the director **n** are free to decouple. The free energy density functions are minimized to reveal coupled differential equations which describe **a** and **n**. Comments are made on cylindrical systems where splay energies are negligible. Solutions are given and the results discussed.

PACS numbers: 61.30.−v, 61.30.Hn, 61.30.Dk

1. Introduction

Liquid crystals are anisotropic fluids made up of elongated molecules which have an average molecular axis that aligns along a common direction in space which is usually denoted by the unit vector **n**, called the director. Smectic liquid crystals are layered structures with a well-defined interlayer distance. These layers may be described by a scalar function Φ, whereby the layer normal is given by $\mathbf{a} = \nabla\Phi/|\nabla\Phi|$. There are many different types of smectic liquid crystals, however this paper shall only concern smectic A. In equilibrium, smectic A liquid crystals form locally equidistant parallel layers in which the director **n** is parallel to the local unit layer normal **a** [5, 17]. However, in both equilibrium and non-equilibrium circumstances, it is believed that the director **n** and the layer normal **a** may decouple [2, 3, 13, 14, 19]. This paper studies this decoupling in two theoretical experiments where cylindrically layered smectic A liquid crystals have imposed director tilt on the boundaries.

To begin with in section 2, we provide a novel method for constructing a nonlinear form of the smectic layer function Φ for Cartesian and cylindrical coordinates. This nonlinear layer function is then used to calculate the free energy density for a smectic A liquid crystal in a cylindrical domain, where the smectic layer normal **a** can decouple from the director **n**. This

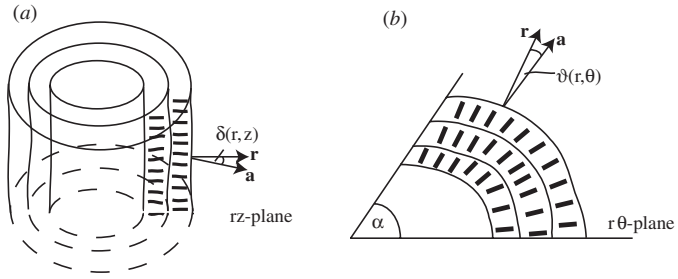

Figure 1. (*a*) A sample of cylindrically layered smectic A where the layer normal makes and angle $\delta(r, z)$ with the r-direction in the rz-plane. (*b*) The corresponding scenario when the layer normal makes an angle $\vartheta(r, \theta)$ with the r-direction in the $r\theta$-plane and the sample is confined across a 'wedge' with planar boundary plates separated by an angle α.

involves using the method of characteristics [9] to solve partial differential equations arising from the condition $\mathbf{a} = \nabla\Phi/|\nabla\Phi|$.

Two theoretical situations, schematically described in figure 1, are studied. The first theoretical experiment involves a cylindrically layered smectic liquid crystal bounded between two glass plates at $z = 0$ and $z = d$, similar to the typical 'bookshelf' geometry in which the planar smectic layers are perpendicular to parallel boundary plates. This get-up is described in figure 1(*a*). The second situation, described in figure 1(*b*), involves a smectic liquid crystal bounded by an infinite cylindrical wedge of angle α. We assume strong anchoring of the director on the boundary plates in both theoretical experiments and also assume that the smectic layers exhibit a fixed layer tilt on the boundary.

In section 3, equilibrium equations for the layer normal **a** and the director **n** are obtained by minimizing the energy integral constructed for the two described situations. The energy density used by Stewart [18, 19] and De Vita and Stewart [6] shall be employed here. This elementary energy density is based upon the work of Auernhammer *et al* [2–4], E [7], Ribotta and Durand [13] and Soddemann *et al* [14]. It takes the form

$$w = \tfrac{1}{2}K_1^a(\nabla\cdot\mathbf{a})^2 + \tfrac{1}{2}K_1^n(\nabla\cdot\mathbf{n})^2 + \tfrac{1}{2}B_0(|\nabla\Phi| + \mathbf{a}\cdot\mathbf{n} - 2)^2 + \tfrac{1}{2}B_1(1 - (\mathbf{n}\cdot\mathbf{a})^2), \tag{1.1}$$

with the total bulk energy being given by

$$W = \int_V w\,\mathrm{d}V, \tag{1.2}$$

where V is the sample volume. In the above expression for the energy density, K_1^n represents the usual elastic splay deformation of the director **n** while K_1^a is a measure of the bending of the smectic layers; both K_1^n and K_1^a are positive elastic constants. The term B_0 is related to smectic layer compression and is an extended version of that which is known for smectic A, based upon the results in [5, 7]. The fourth term is a measure of the strength of the coupling between **a** and **n** with the positive constant B_1 having dimensions of energy per unit volume. We note that in an equilibrium situation this contribution to the energy is minimized when the director and the layer normal are parallel. The last term is essentially $B_1(\mathbf{n}\times\mathbf{a})^2$, which was first proposed by Auernhammer *et al* [2]. The energy density (1.1) is invariant under the simultaneous changes in sign $\mathbf{n}\to-\mathbf{n}$ and $\mathbf{a}\to-\mathbf{a}$, which is equivalent to invariance under the simultaneous changes $\mathbf{n}\to-\mathbf{n}$ and $\nabla\Phi\to-\nabla\Phi$.

In sections 3.1 and 3.2, the equilibrium equations for both theoretical experiments are solved numerically to obtain the two angles which define the layer normal and the director. It is shown in section 3.1 that the situation described schematically in figure 1(*a*) is analogous to

a planar-layered case [19] when layers of large radius are studied. A specific case where the layer compression is assumed to be the driving force of the realignment of the director and layer normal is then considered in section 4. Comments are made on the results obtained in section 5. Specific mention is made on the form of the free energy density used and the scope for further investigations on the smectic layer function and in turn the smectic layer normal.

2. Nonlinear layer functions

We present here a novel method for constructing a nonlinear form of the smectic layer function Φ for Cartesian and cylindrical coordinates. In many previous cases, a linear form of the layer function Φ is assumed with possible nonlinear components. For example, the layer function given by $\Phi = x + u(x, y, z, t)$ would describe planar layers with a possible displacement of the layers described by the term $u(x, y, z, t)$, which could be nonlinear. Similar forms have been used previously [5, 13 , 15–17]. Additionally, the layer function $\Phi = r + u(r, \theta, z, t)$ would describe cylindrical layers with some possible deformation $u(r, \theta, z, t)$. This form has also been used previously [10, 22].

From a geometrical argument, the layer normal $\mathbf{a}$ and the layer function Φ are related by the equation

$$\mathbf{a} = \frac{\nabla\Phi}{|\nabla\Phi|}. \tag{2.1}$$

This equation provides us with, at most three partial differential equations relating the layer function Φ and the layer normal $\mathbf{a}$.

2.1. Cartesian case

Assume, for the moment, that we have a planar-layered smectic A under some stress which is large enough to cause layer undulations. Here the layer normal and the director are assumed to not be always coincident. We denote by δ the angle the layer normal makes with the z-direction and ζ the angle the director makes with the z-direction. Assuming no y-dependence in the angles which describe the vectors $\mathbf{a}$ and $\mathbf{n}$, it follows that the layer normal and the director would take the forms, respectively,

$$\mathbf{a} = (\sin(\delta(x, z)), 0, \cos(\delta(x, z))), \tag{2.2}$$

$$\mathbf{n} = (\sin(\zeta(x, z)), 0, \cos(\zeta(x, z))). \tag{2.3}$$

When $\zeta \equiv \delta \equiv 0$, we have the usual level sets of undisturbed planar-layered smectic A, i.e. $\mathbf{a} \equiv \mathbf{n} \equiv (0, 0, 1)$. However, as previously noted, $\mathbf{a} = \nabla\Phi/|\nabla\Phi|$, and so we may uncover the following partial differential equations arising via (2.1) and (2.2), namely

$$\frac{\Phi_{,x}}{|\nabla\Phi|} = \sin(\delta(x, z)), \tag{2.4}$$

$$\frac{\Phi_{,y}}{|\nabla\Phi|} = 0, \tag{2.5}$$

$$\frac{\Phi_{,z}}{|\nabla\Phi|} = \cos(\delta(x, z)). \tag{2.6}$$

Of course, we immediately see from equation (2.5) that $\Phi_{,y} \equiv 0$, i.e. the layer function is not dependent on the spatial variable y, which is to be expected since it was assumed that the

layer normal was not dependent on y. Since $\cos(\delta(x, z))$ is expected to be nonzero (i.e. delta not close to $\pi/2$) we can divide the right-hand side of equation (2.4) by the right-hand side of equation (2.6). To maintain equality we divide the left-hand side of equation (2.4) by the left-hand side of equation (2.6), which then reveals the relation

$$\frac{\Phi_{,x}}{\Phi_{,z}} = \frac{\sin\delta}{\cos\delta}. \tag{2.7}$$

Employing this method forces the constraint $\Phi_{,z} \neq 0$ (for $0 < \delta < \pi/2$), i.e. the layer function Φ must at least be a function of the spatial variable z. This is to be expected physically and hence we can continue to write the above partial differential equation in the form

$$\Phi_{,x} - \tan(\delta(x, z))\Phi_{,z} = 0, \tag{2.8}$$

which can be solved using the method of characteristics given that we assume $\delta = \delta(x)$. This is a valid assumption in the planar-layered case as can be seen by the experimental work of Elston [8] and the theoretical work of Stewart [18] where there is no z-dependence of the layer normal across the layers (perpendicular to the layers). The solution to equation (2.8) is given by

$$\Phi = F\left(z + \int_{x_0}^{x} \tan\delta(t)\mathrm{d}t\right), \tag{2.9}$$

where F is an arbitrary function and $x_0 = x(0)$. Of course, care must be taken here since the layer function must have dimensions of distance. It seems that while equation (2.9) is a mathematical solution to the physical situation described by equations (2.1) and (2.2), it may not necessarily be a physically realistic solution. For example, consider the case when there is no variation to the layer structure, that is $\delta(z) = 0$. We expect the layer function to be of the form $\Phi = z$. However, we find ourselves faced with the solution $\Phi = F(z)$ which, for any function other than $F(z) = z$, would result in a surprising layer structure. Hence, it is intuitive to write the layer function in the form

$$\Phi = z + \int_{x_0}^{x} \tan\delta(t)\,\mathrm{d}t. \tag{2.10}$$

This form for the layer function was first used by Stewart [19].

This technique can also be used to find a nonlinear form of the layer function in a cylindrical domain, as illustrated in the following section.

2.2. *Cylindrical case*

We now consider a smectic A liquid crystal with cylindrical layers in two different situations, as shown in figure 1. If the layer normal makes an angle $\delta(r, z)$ in the rz-plane, as shown in figure 1(*a*), then the layer normal would take the form

$$\mathbf{a} = (\cos\delta(r, z), 0, \sin\delta(r, z)), \tag{2.11}$$

and emulating the procedure described in the previous section, the corresponding partial differential equation for the layer function would be

$$\Phi_{,z} - \tan(\delta)\Phi_{,r} = 0. \tag{2.12}$$

If the layer normal makes an angle $\vartheta(r, \theta)$ with the radial direction in the $r\theta$-plane, as shown in figure 1(*b*), then the corresponding equations would be

$$\mathbf{a} = (\cos\vartheta(r, \theta), \sin\vartheta(r, \theta), 0), \tag{2.13}$$

$$\Phi_{,\theta} - r\tan(\vartheta)\Phi_{,r} = 0. \tag{2.14}$$

The solutions to the partial differential equations given here can only be found by the method of characteristics given that we assume dependence of only one variable in the angle which describes the layer function. Following from [8], and the assumption made above, we assume that all angles are dependent only on the variable which is parallel to the smectic layers, i.e. $\vartheta = \vartheta(\theta)$ and $\delta = \delta(z)$. The solutions to the partial differential equations (2.12) and (2.14) are then given by, respectively,

$$\Phi = F_1\left(r + \int_{z_0}^{z} \tan\delta(t)\,\mathrm{d}t\right), \tag{2.15}$$

$$\Phi = F_2\left(r\exp\int_{\theta_0}^{\theta} \tan\vartheta(t)\,\mathrm{d}t\right), \tag{2.16}$$

where F_1 and F_2 are arbitrary functions, $z_0 = z(0)$ and $\theta_0 = \theta(0)$. All of the above formulations hold when $\delta = 0$ (or $\vartheta = 0$), even though the defining partial differential equations do not. Similar systems of partial differential equations can be constructed when the director and the layer normal are defined by two angles of rotation, see [21] for details.

3. Minimization of free energy

We shall now construct the free energy associated with the two situations described in figure 1. Once constructed, we find in each case, two coupled ordinary differential equations. In the first instance, where we consider the situation described in figure 1(*a*), the equations can be manipulated at layers of large radius to emulate those found for a similar planar-layered smectic A system [18]. The corresponding Euler–Lagrange equations are solved numerically and comments are made on the solutions with respect to the planar-layered case. A similar free energy and corresponding Euler–Lagrange equations are constructed for the system described in figure 1(*b*). The equations are solved and comments are made on the solutions.

3.1. Layers in the rz-plane

We consider a cylindrically layered sample of smectic A liquid crystal confined between two plates at $z = 0$ and $z = d$, where the smectic layer normal makes an angle $\delta(z)$ with the radial coordinate in the rz-plane. We assume that the director makes an angle $\zeta(z)$ with the radial direction in the rz-plane. Strong anchoring of the director will be supposed and therefore we will set ζ to be the fixed angle ζ_0 at the lower boundary $z = 0$ and $-\zeta_0$ at the upper boundary at $z = d$. We expect the director angle to vary smoothly from ζ_0 to $-\zeta_0$ due to the requirement of minimization of splayed energy [8] and hence we expect $\zeta(d/2) = 0$. It will also be assumed that the smectic layers will exhibit a fixed layer tilt δ_0 at $z = 0$ and $-\delta_0$ at $z = d$ and the further assumption is made that the layer tilt angle varies smoothly. A further discussion on this assumption of the tilt of the smectic layers on the boundaries is made in section 5. These assumptions are concurrent with the experimental findings of Elston [8] and the theoretical investigations of Stewart [18] for planar-layered smectic liquid crystals.

The layer normal and layer function are given for this problem by equations (2.11) and (2.16), respectively. The director can be written in the form

$$\mathbf{n} = (\cos\zeta(z), 0, \sin\zeta(z)). \tag{3.1}$$

Inserting equations (2.11), (2.15) and (3.1) into (1.1) results in the energy density

$$w_A = \frac{1}{2}K_1^a\left(\frac{1}{R}\cos\delta + \delta_{,z}\cos\delta\right)^2 + \frac{1}{2}K_1^n\left(\frac{1}{R}\cos\zeta + \zeta_{,z}\cos\zeta\right)^2 + \frac{1}{2}B_0\left(\sec\delta + \cos(\zeta-\delta) - 2\right)^2 + \frac{1}{2}B_1\sin^2(\zeta-\delta), \tag{3.2}$$

where the fixed number R is the radius of any particular layer being studied. Inserting (3.2) into the Euler–Lagrange equations

$$\frac{\partial w}{\partial \zeta} - \frac{\mathrm{d}}{\mathrm{d}z}\left(\frac{\partial w}{\partial \zeta_{,z}}\right) = 0 \tag{3.3}$$

$$\frac{\partial w}{\partial \delta} - \frac{\mathrm{d}}{\mathrm{d}z}\left(\frac{\partial w}{\partial \delta_{,z}}\right) = 0 \tag{3.4}$$

results in the following two coupled ordinary differential equations:

$$K_1^n\left(\frac{1}{R^2}\sin\zeta\cos\zeta + \zeta_{,zz}\cos^2\zeta - \zeta_{,z}^2\sin\zeta\cos\zeta\right) - B_1\cos(\zeta-\delta)\sin(\zeta-\delta) + B_0(\sec\delta\tan\delta + \cos(\zeta-\delta) - 2)\sin(\zeta-\delta) = 0, \tag{3.5}$$

$$K_1^a\left(\frac{1}{R^2}\sin\delta\cos\delta + \delta_{,zz}\cos^2\delta - \delta_{,z}^2\sin\delta\cos\delta\right) + B_1\cos(\zeta-\delta)\sin(\zeta-\delta) - B_0(\sec\delta\tan\delta + \cos(\zeta-\delta) - 2)(\sec\delta\tan\delta - \sin(\zeta-\delta)) = 0. \tag{3.6}$$

Introducing the variables

$$\kappa = \frac{K_1^a}{K_1^n}, \qquad \lambda = \sqrt{\frac{K_1^n}{B_0}}, \qquad B = \frac{B_1}{B_0}, \qquad \bar{z} = \frac{z}{\lambda}, \qquad \bar{R} = \frac{R}{\lambda}, \qquad \bar{d} = \frac{d}{\lambda}, \tag{3.7}$$

allows us to non-dimensionalize the Euler–Lagrange equations so that they may be written as

$$\left(\frac{1}{\bar{R}^2}\sin\zeta\cos\zeta + \zeta_{,zz}\cos^2\zeta - \zeta_{,z}^2\sin\zeta\cos\zeta\right) - B\cos(\zeta-\delta)\sin(\zeta-\delta) + (\sec\delta\tan\delta + \cos(\zeta-\delta) - 2)\sin(\zeta-\delta) = 0, \tag{3.8}$$

$$\kappa\left(\frac{1}{\bar{R}^2}\sin\delta\cos\delta + \delta_{,zz}\cos^2\delta - \delta_{,z}^2\sin\delta\cos\delta\right) + B\cos(\zeta-\delta)\sin(\zeta-\delta) - (\sec\delta\tan\delta + \cos(\zeta-\delta) - 2)(\sec\delta\tan\delta - \sin(\zeta-\delta)) = 0. \tag{3.9}$$

This choice of non-dimensionalized variables has been chosen in-line with the work by Elston [8] and Stewart [18] and incorporates a molecular length scale identified by de Gennes and Prost [5]. The boundary conditions for these equations are set as

$$\zeta(0) = \zeta_0, \qquad \zeta(\bar{d}) = -\zeta_0, \qquad \delta(0) = \delta_0, \qquad \delta(\bar{d}) = -\delta_0, \tag{3.10}$$

and it is intuitive from the symmetry of the sample to infer

$$\zeta\left(\frac{\bar{d}}{2}\right) = 0, \qquad \delta\left(\frac{\bar{d}}{2}\right) = 0. \tag{3.11}$$

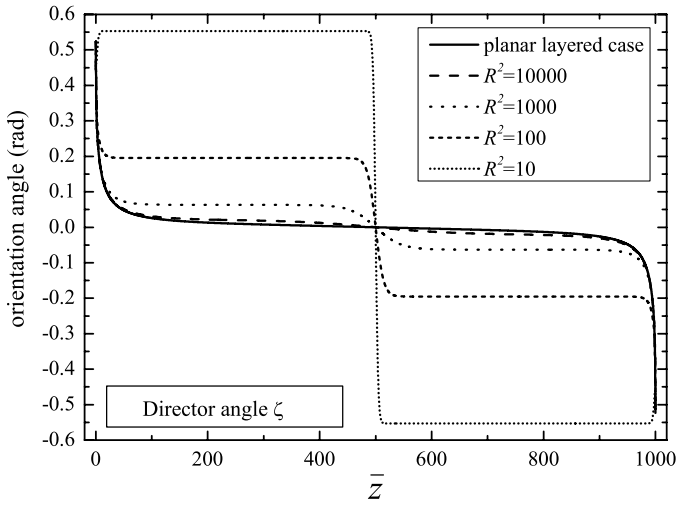

Figure 2. Numerical solutions to equations (3.8), (3.9), (3.13) and (3.14) for the director angle ζ for layers of varying radii $\bar{R}$ and the parameter values $\bar{d} = 1000$, $\zeta_0 = \pi/6$, $\delta_0 = \pi/18$, $B = 1$ and $\kappa = 1$. As the solutions for ζ and δ almost coincide in the bulk of the sample, only the ζ solutions are plotted here. The effects at the boundary for both angles can be seen for layers of varying radii in figure 4 and for varying control parameters in figure 5. We note that the layer normal and director are almost zero (i.e. like smectic A in equilibrium) for most of the bulk.

There are two control parameters for this problem, κ and B, which are dimensionless measures of the relative elasticities and ratio of coupling to compression. First, we consider the case $R \to \infty$, i.e. when the cylindrical layers are locally planar. Here the energy density becomes

$$w_A = \tfrac{1}{2}K_1^n \zeta_{,z}^2 \cos^2\zeta + \tfrac{1}{2}K_1^a \delta_{,z}^2 \cos^2\delta + \tfrac{1}{2}B_0(\sec\delta + \cos(\zeta-\delta) - 2)^2 + \tfrac{1}{2}B_1 \sin^2(\zeta-\delta), \tag{3.12}$$

and the associated Euler–Lagrange equations in dimensionless form are

$$\zeta_{,zz}\cos^2\zeta - \zeta_{,z}^2 \sin\zeta\cos\zeta - B\sin(\zeta-\delta)\cos(\zeta-\delta) + (\sec\delta + \cos(\zeta-\delta) - 2)\sin(\zeta-\delta) = 0, \tag{3.13}$$

$$\kappa(\delta_{,zz}\cos^2\delta - \delta_{,z}^2 \sin\delta\cos\delta) + B\sin(\zeta-\delta)\cos(\zeta-\delta) - (\sec\delta + \cos(\zeta-\delta) - 2)(\sec\delta\tan\delta + \sin(\zeta-\delta)) = 0, \tag{3.14}$$

which are analogous equations to those proposed for planar smectic A liquid crystals in planar layers [18]. Using the above planar-like equations, and the equations for cylindrical layers of various radii, we solve numerically for given values of B, κ, ζ_0, δ_0, $\bar{R}$ and $\bar{d}$ using the mathematics software package MAPLE [11] which uses a finite difference technique with Richardson extrapolation (see [1] for further information on Richardson extrapolation). Figure 2 shows solutions of equations (3.8) and (3.9) (for finite $\bar{R}$) and equations (3.13) and (3.14) (the planar case) for the angle which defines the director, ζ, when, for typical values (see Elston [8] and Stewart [18]) $\bar{d} = 1000$, $\kappa = 1$, $B = 1$, $\zeta_0 = \pi/6$ and $\delta_0 = \pi/18$, for varying magnitudes of $\bar{R}$, as well as when $\bar{R} \to \infty$. We choose this value of $\bar{d}$ so that the boundary layer phenomena can be clearly illustrated. For macroscopic samples, we would

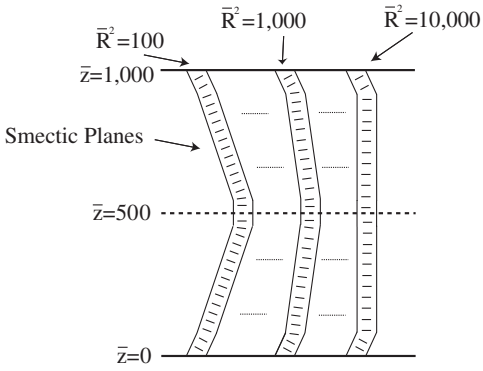

Figure 3. Schematic diagram of the results presented in figure 2. Here, we have presented a cut-view of the sample in the rz-plane ($\theta \equiv 0$). We note the chevron structure which arises due to the imposed boundary conditions, which is more prominent for layers of small radius.

require $\bar{d} > 10^6$ which would only increase the complexity of the numerical problem and would not provide further information on the boundary layer effects. As δ closely resembles ζ in the central bulk of the sample (similar to the results in [18]) we omit its solution at this stage and defer a discussion of the differences between these angles to the results below. We see that for very large values of $\bar{R}$, the sample closely resembles that of the planar-layered case investigated in [18], that is, ζ and δ are close to zero across the bulk of the sample. However, when the layers of lower radius are studied, the angles across the bulk quite far away from zero. We note especially the shape of the solution at $\bar{R}^2 = 10$, which shows that the layer normal angle ζ actually increases close to the boundary. As yet, it is unclear if this would occur experimentally. It may be an indication that the dynamic theory is breaking down at such a small value of the radius of the layer studied. We note that $\bar{R}^2 = 10$ indicates a layer of radius around 10^{-9} m which is just below the common range for average smectic layer thickness of 20–30 Å. Since the core radius of liquid crystals is usually estimated to be of the order of molecular dimensions [17, p 113], we may assume that layers of radius $\bar{R}^2 = 10$ may not exist in experimental conditions and therefore the solution for $\bar{R}^2 = 10$ may be considered purely mathematical.

The results presented in figure 2 are sketched for clarity in figure 3. We note the chevron structure of the smectic layers which arise due to the imposed boundary conditions and the dependence of the radius. This provides evidence on the requirement that the layer normal and the director must have a mathematical dependence on the radius r in addition to the spatial variable z.

Figure 4 shows four comparison plots of the boundary layer phenomena for the planar-layered case and when the layers of radii $\bar{R}^2 = 10000$, $\bar{R}^2 = 1000$, and $\bar{R}^2 = 100$ are studied. The plots are over a log scale on $[0, 500]$ to emphasize the features of the uncoupled behaviour of δ and ζ. In all cases, ζ and δ first become close over a relatively small distance of $\bar{z} = 1$–5. Nevertheless, it is clear that the layer normal and director do not get as close in layers of small radius as they do for layers of large radius. The layer structure is seen to be extremely dependent on the radius, as it gets close to the typical smectic A alignment ($\delta \approx 0$) at very different values of $\bar{z}$, for different values of $\bar{R}$. Note in the $\bar{R}^2 = 10$ case that the layer normal and director do not meet until midway through the bulk. They both settle in the main part at angles greater than those imposed by the boundary conditions. Again, we

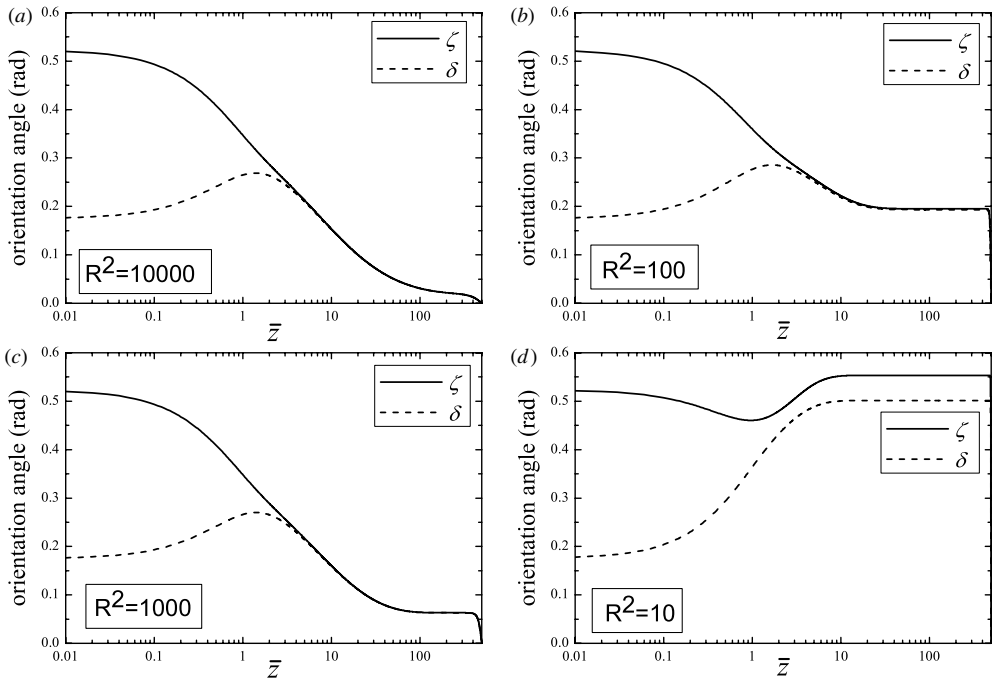

Figure 4. Solutions to equations (3.8), (3.9), with the boundary conditions (3.10), for $\delta(z)$ (dashed lines) and $\zeta(z)$ (solid lines) for the indicated values of the radius $\bar{R}$ of the layers being studied. The remaining parameters have been set as $\bar{d} = 1000$, $\zeta_0 = \pi/6$, $\delta_0 = \pi/18$, $B = 1$ and $\kappa = 1$. The plots are over a log scale on [0, 500] to emphasize the features of the uncoupled behaviour of δ and ζ. Discussion of observations can be found in the main text.

remark that this is unlikely to be a physical solution as layers of this magnitude may not exist experimentally.

Figure 5 shows four comparison plots of the boundary layer phenomena when the material parameters B and κ are altered. We note the dependence of the solutions upon the dimensionless elastic control parameter κ. If κ is small, i.e. $K_1^n > K_1^a$, then the layer angle δ increases so that the layer normal is parallel to the director. However, if κ is large, i.e. $K_1^a > K_1^n$, then the layers remain fixed at their boundary states until the director has reoriented to be parallel to the layer normal, they then both reorient to the equilibrium state $\delta = \zeta = 0$. The size of the parameter κ also determines where the angles prefer to align to in the main of the bulk. Given a large κ, the layers and the director prefer to settle in a tilted state quite far from $\zeta = \delta = 0$. These results can be explained physically; when we consider a large κ then we are actually considering that the layers are less free to move than the director, and vice versa. For small values of B, i.e. $B_0 > B_1$, the director does not realign to be parallel to the layer normal until further into the bulk. This can be related to the minimization of the coefficient of B_0, i.e. the minimization of $(|\nabla\Phi| + \mathbf{n}\cdot\mathbf{a} - 2)$. For large values of B, the angles defining the director and layer normal are forced to become closer.

Using the information supplied in the numerical solutions to the Euler–Lagrange equations, we can find the integrated angle of inclination across the domain wall, w_d, for smectic layers at different radius. The domain walls are centred at $\bar{z} = 500$ and we consider the difference in the values of ζ (or δ) at the positions $z = d/4$ and $z = 3d/4$. Figure 6 shows

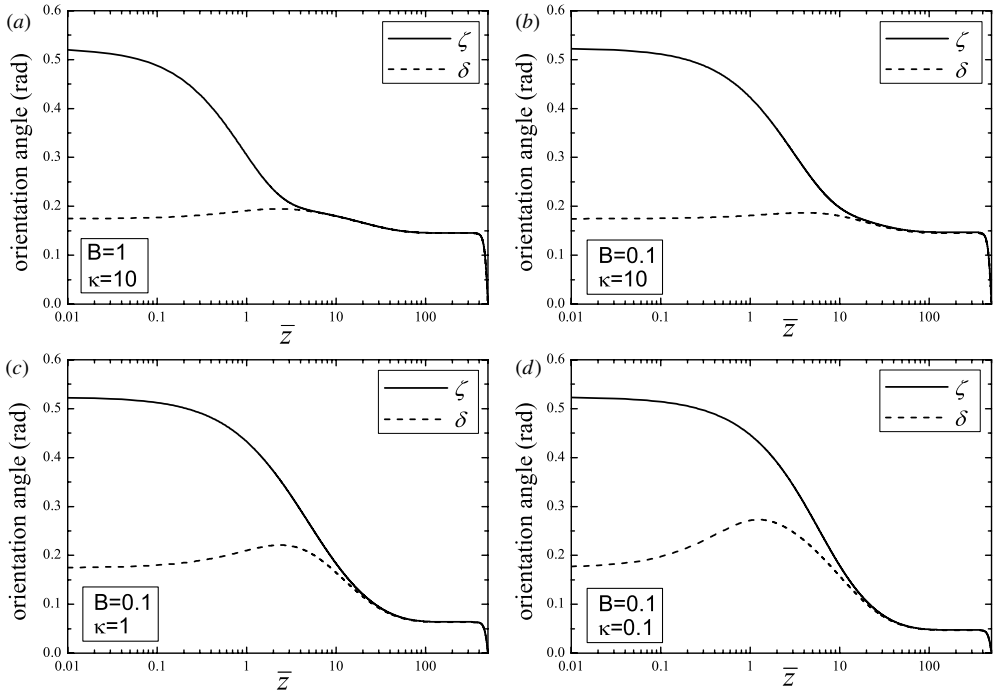

Figure 5. Solutions to equations (3.8), (3.9), with the boundary conditions (3.10), for $\delta(z)$ (dashed lines) and $\zeta(z)$ (solid lines) for the layers of radius around $\bar{R}^2 = 1000$ and indicated values of the control parameters B and κ. The remaining parameters have been set as $\bar{d} = 1000$, $\zeta_0 = \pi/6$ and $\delta_0 = \pi/18$. Discussion of observations can be found in the main text.

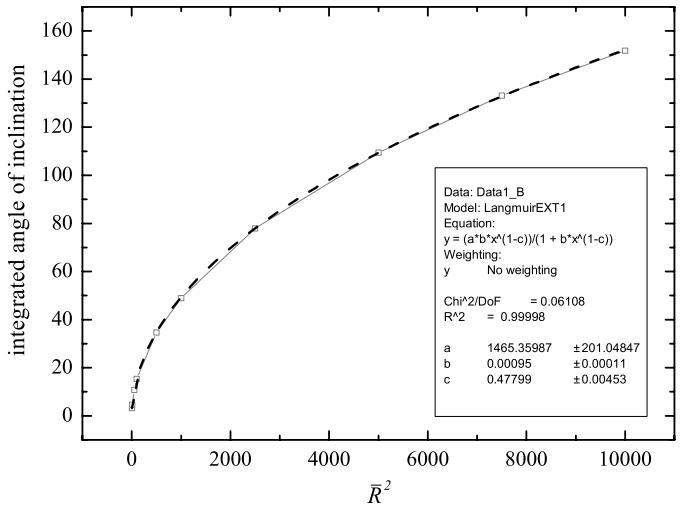

Figure 6. Plot and fitting curve of the integrated angle of inclination across the domain wall as a function of the radius of the layers begin investigated. We see that this angle can be estimated to a very good accuracy (the chi-squared test resulting in a p value of $\approx$0.06) by a simple function given by equation (3.15).

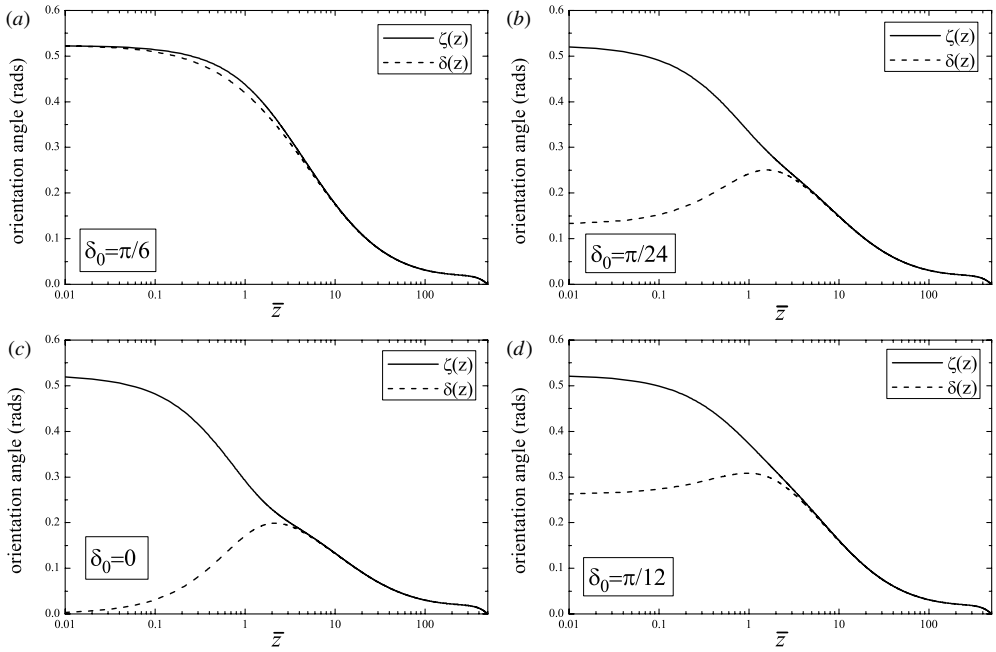

Figure 7. Solutions to equations (3.8), (3.9), with the boundary conditions (3.10), for $\delta(z)$ (dashed lines) and $\zeta(z)$ (solid lines) for the layers of radius around $\bar{R}^2 = 1000$ and indicated boundary values. The remaining parameters have been set as $\bar{d} = 1000$, $B = 1$ and $\kappa = 1$. Discussion of observations can be found in the main text.

the result of this analysis. We see quite clearly using a fitting program [12] that the length of the domain wall can be estimated to a very good accuracy (the chi-squared test resulting in a p value of $\approx$0.06) by the following simple ratio of powers:

$$w_d \approx \frac{ab\bar{R}^{2(1-c)}}{1 + b\bar{R}^{2(1-c)}}, \tag{3.15}$$

where

$$a = 1465.359\,87 \pm 201.04847, \quad b = 0.000\,95 \pm 0.00011, \quad c = 0.477\,99 \pm 0.00453. \tag{3.16}$$

We see that at layers of small radius the domain wall width is very small and increases in length as layers of larger radius are considered. It could be argued that for layers of small radius, the imposed symmetry of the system is forcing the angles to reorient to zero in the middle of the bulk, when they may not do so experimentally. It remains to be seen whether or not this is the case, or indeed whether or not layers of such small radius could exist. It is unclear at the moment if the form of equation (3.15) is coincidental or whether there exists some underlying structure driving its form.

We investigate also what happens to the layers and the director when different boundary conditions are applied. In figure 7 we consider the problem described above, and look at the layers around $\bar{R}^2 = 1000$ when the layer normal boundary condition is fixed at $\zeta_0 = \pi/6$. Four different boundary conditions are considered for the director: $\delta_0 = \pi/6$, $\delta_0 = \pi/12$, $\delta_0 = \pi/24$ and $\delta_0 = 0$. We see in the first instance where $\delta_0 = \zeta_0 = \pi/6$, that even if the two angles have the same boundary value, they decouple almost immediately, only to realign within a relatively short distance from the boundary. This also occurs to some extent in the

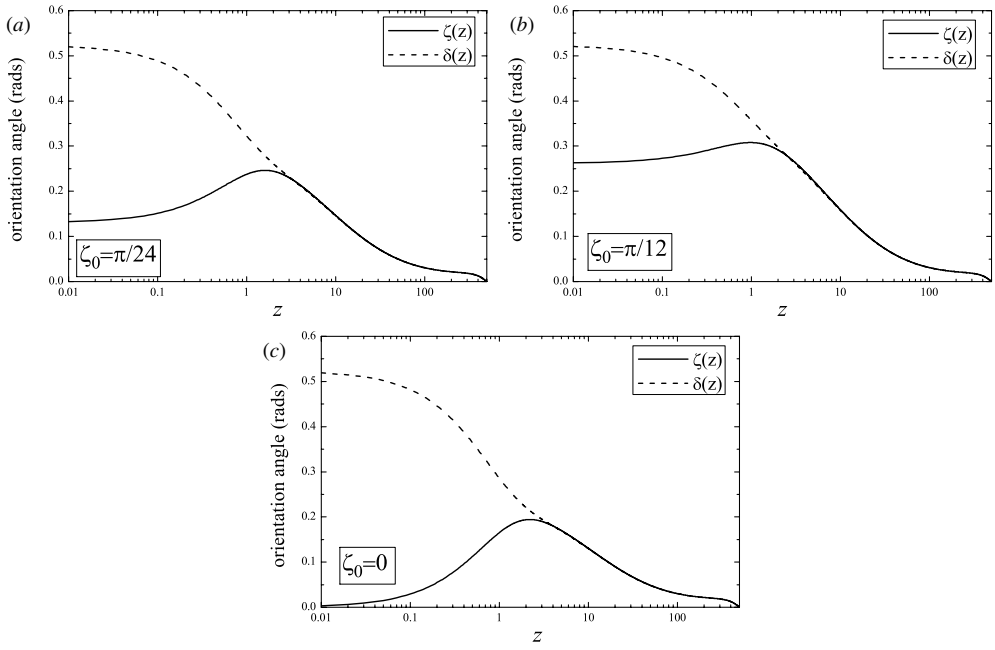

Figure 8. Solutions to equations (3.8), (3.9), with the boundary conditions (3.10), for $\delta(z)$ (dashed lines) and $\zeta(z)$ (solid lines) for the layers of radius around $\bar{R}^2 = 1000$ and indicated boundary values. The remaining parameters have been set as $\bar{d} = 1000$, $B = 1$ and $\kappa = 1$. Discussion of observations can be found in the main text.

planar-layered case when the boundary conditions are set to be equal. It is also noticeable that the angles realign around the same value of $\bar{z}$, no matter how far apart their boundary values are.

Figure 8 tells a similar story with δ_0 fixed with three different values of ζ_0. In parts (a), (b) and (c) we have set $\delta_0 = \pi/6$ and $\zeta_0 = \pi/24$, $\zeta_0 = \pi/12$ and $\zeta_0 = 0$, respectively. Similar to the results seen from figure 7, the angles all realign around the same value of $\bar{z}$. Numerical calculations were made when $\delta_0 = 0$ and $\zeta_0 = 0$, as expected both angles remain fixed at their boundary state.

3.2. Layers in the $r\theta$-plane

Here we consider the situation described in figure 1(b), a cylindrically layered sample of smectic A, confined between two glass plates at some angle α, where the layer normal makes an angle $\vartheta(\theta)$ with the radial coordinate in the $r\theta$-plane. We assume that the director makes an angle $\zeta(\theta)$ with the radial coordinate in the $r\theta$-plane. Analogous to the previous case, we shall assume a boundary at $\theta = 0$ and another boundary at $\theta = \alpha$, for some fixed angle α. Strong anchoring of the director will be supposed and therefore we shall set ζ to be the fixed angle ζ_0 at $\theta = 0$ and $-\zeta_0$ at $\theta = \alpha$. It will also be assumed that the smectic layers will exhibit a fixed layer tilt ϑ_0 at $\theta = 0$ and $-\vartheta_0$ at $\theta = \alpha$.

The layer normal and the layer function are given by equations (2.13) and (2.16). From figure 1(b), the director can be written in the form

$$\mathbf{n} = (\cos\zeta(\theta), \sin\zeta(\theta), 0). \tag{3.17}$$

We note here that we have an *a priori* restriction on both $\vartheta(\theta)$ and $\zeta(\theta)$ in that they must both be 2π-periodic.

Using the form for the free energy of a smectic A liquid crystal with variable layers given by equation (1.1), the free energy for this system can be written as

$$\begin{aligned} w_A = {} & \frac{1}{2R^2} K_1^n \cos^2\zeta (1+\zeta_{,\theta})^2 + \frac{1}{2R^2} K_1^a \cos^2\vartheta (1+\vartheta_{,\theta})^2 \\ & + \frac{1}{2} B_0 \left(\exp\left(\int_{\theta_0}^{\theta} \tan\vartheta(t)\,\mathrm{d}t \right) \sec\vartheta + \cos(\zeta-\vartheta-2) \right)^2 \\ & + \frac{1}{2} B_1 \sin^2(\zeta-\vartheta), \end{aligned} \tag{3.18}$$

where R is the radius of the layers being studied. Inserting (3.18) into the Euler–Lagrange equations

$$\frac{\partial w}{\partial \zeta} - \frac{\mathrm{d}}{\mathrm{d}\theta}\left(\frac{\partial w}{\partial \zeta_{,\theta}} \right) = 0 \tag{3.19}$$

$$\frac{\partial w}{\partial \vartheta} - \frac{\mathrm{d}}{\mathrm{d}\theta}\left(\frac{\partial w}{\partial \vartheta_{,\theta}} \right) = 0 \tag{3.20}$$

results in the following two coupled ordinary differential equations in dimensionless form:

$$\begin{aligned} & \frac{1}{\bar{R}^2}(\zeta_{,\theta\theta}\cos^2\zeta + \sin\zeta\cos\zeta(1-(\zeta_{,\theta})^2)) - B\sin(\zeta-\vartheta)\cos(\zeta-\vartheta) \\ & \quad + \sin(\zeta-\vartheta)\left(\exp\left(\int_{\theta_0}^{\theta} \tan\vartheta(t)\,\mathrm{d}t \right) \sec\vartheta + \cos(\zeta-\vartheta) - 2 \right) = 0, \end{aligned} \tag{3.21}$$

$$\begin{aligned} & \frac{1}{\bar{R}^2}\kappa(\vartheta_{,\theta\theta}\cos^2\vartheta + \sin\vartheta\cos\vartheta(1-(\vartheta_{,\theta})^2)) + B\sin(\zeta-\vartheta)\cos(\zeta-\vartheta) \\ & \quad - \left(\exp\left(\int_{\theta_0}^{\theta} \tan\vartheta(t)\,\mathrm{d}t \right) \sec\vartheta + \cos(\zeta-\vartheta) - 2 \right) \\ & \quad \times \left(\exp\left(\int_{\theta_0}^{\theta} \tan\vartheta(t)\,\mathrm{d}t \right) (\sec^2\vartheta + \sec\vartheta\tan\vartheta) + \sin(\zeta-\vartheta) \right) = 0, \end{aligned} \tag{3.22}$$

where the variables

$$\kappa = \frac{K_1^a}{K_1^n}, \qquad \lambda = \sqrt{\frac{K_1^n}{B_0}}, \qquad B = \frac{B_1}{B_0}, \qquad \bar{R} = \frac{R}{\lambda} \tag{3.23}$$

have been utilized in order to non-dimensionalize. These equations are analogous to equations (3.8) and (3.9). Note that for layers of large radius $\bar{R}$, where the layers are locally planar, elastic contributions are negligible. Unfortunately, due to the existence of the exponential term, solutions to equations (3.21) and (3.22) are intractable. Nevertheless, assuming the layer normal angle ϑ is small allows us to use the approximation

$$\exp\left(\int_{\theta_0}^{\theta} \tan\vartheta(t)\,\mathrm{d}t \right) \approx 1. \tag{3.24}$$

Consequently, the defining differential equations can be simplified to give

$$\begin{aligned} & \frac{1}{\bar{R}^2}(\zeta_{,\theta\theta}\cos^2\zeta + \sin\zeta\cos\zeta(1-(\zeta_{,\theta})^2)) - B\sin(\zeta-\vartheta)\cos(\zeta-\vartheta) \\ & \quad + \sin(\zeta-\vartheta)(\sec\vartheta + \cos(\zeta-\vartheta) - 2) = 0, \end{aligned} \tag{3.25}$$

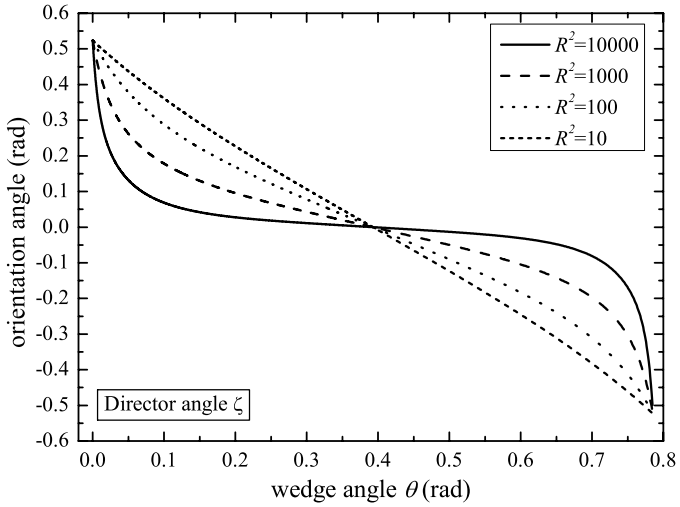

Figure 9. Numerical solutions to equations (3.25) and (3.26) for the director angle ζ for layers of varying radius $\bar{R}$ and the parameter values $\alpha = \pi/4$, $\zeta_0 = \pi/6$, $\vartheta_0 = \pi/18$, $B = 1$ and $\kappa = 1$. In layers of large radius, which are locally planar, the director angle aligns to $\zeta \approx 0$ in the bulk, yet at layers of small radius the orientation of the director from one boundary to the other is almost linear.

$$\frac{1}{\bar{R}^2}\kappa(\vartheta_{,\theta\theta}\cos^2\vartheta + \sin\vartheta\cos\vartheta(1-(\vartheta_{,\theta})^2)) + B\sin(\zeta-\vartheta)\cos(\zeta-\vartheta) - (\sec\vartheta + \cos(\zeta-\vartheta) - 2)((\sec^2\vartheta + \sec\vartheta\tan\vartheta) + \sin(\zeta-\vartheta)) = 0, \quad (3.26)$$

which can be solved in a similar manner to those in the previous section. Given the boundary conditions

$$\vartheta(0) = \vartheta_0, \qquad \vartheta(\alpha) = -\vartheta_0, \qquad \zeta(0) = \zeta_0, \qquad \zeta(\alpha) = -\zeta_0, \quad (3.27)$$

we solve numerically for given values of B, κ, ϑ_0, ζ_0 and a fixed range of values for $\bar{R}$. The wedge angle α shall not be varied and is set to be $\alpha = \pi/4$. Figure 9 gives the solutions for ζ and ϑ when $\vartheta_0 = \pi/18$, $\zeta_0 = \pi/6$, $B = 1$, $\kappa = 1$ and for varying values of the layer radius $\bar{R}$. We find that for layers of large radius $\bar{R}$, which are locally planar, the director quickly realigns to $\zeta \approx 0$ in the bulk. However, when layers of small radius are studied, the orientation of the director from one boundary to another is almost linear. We also find that the layers try to align themselves with the director. Consequently, layer tilt actually increases close to the boundary. We see this effect is greater in layers of large radius. Since the layers attempt to realign to have a layer normal parallel to the director, the layers also realign close to an equilibrium state in the bulk and yet are forced into a linear orientation from one boundary value to the other at low radius. A sketch of the solutions presented in figures 9 and 10 is given via figure 11. We note that the angle which defines the layer normal actually increases close to the boundaries before realigning close to zero in the main of the bulk.

Figure 12 shows four comparison plots of the boundary layer phenomena when the layers of radii $\bar{R}^2 = 10000$, $\bar{R}^2 = 1000$, $\bar{R}^2 = 100$ and $\bar{R}^2 = 10$ are studied. It is clear that the layer normal and director do not coalesce as readily in layers of small radius as they do for layers of large radius. When layers of large radius are studied, we find that the layers reorient away from the smectic A equilibrium state, in order to align with the director, before reorienting

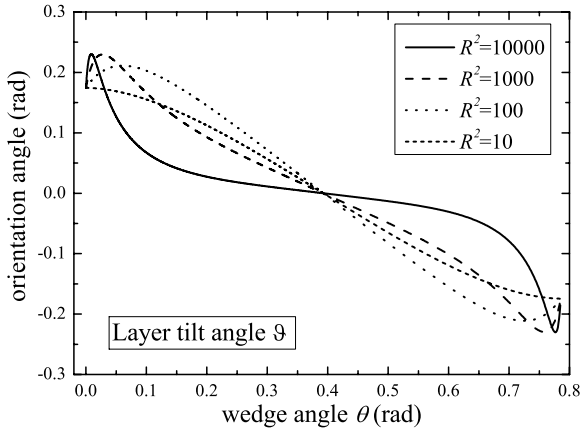

Figure 10. Numerical solutions to equations (3.25) and (3.26) for the layer tilt angle ϑ for layers of varying radius $\bar{R}$ and the parameter values $\alpha = \pi/4$, $\zeta_0 = \pi/6$, $\vartheta_0 = \pi/18$, $B = 1$ and $\kappa = 1$. Note how the radius of the layers affects the orientation on the layers. Layers of large radius, which are locally planar, reorient to a typical smectic A formation much easier than layers of small radius.

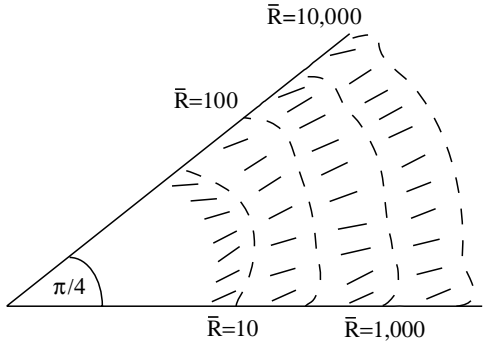

Figure 11. Sketch of the results presented in figures 9 and 10 where the dashed lines denote the smectic layers and the short solid lines denote the director. Note the unusual behaviour of the layers close to the boundaries.

towards the zero state. That is, the angle ϑ actually increases towards ζ_0 to align with ζ before decreasing with ζ to $\vartheta = \zeta = 0$. However, when layers of small radius are studied, the layers remain fixed until the director reorients in line with them before reorienting towards the equilibrium state.

Figure 13 shows four comparison plots of the boundary layer phenomena when the material parameters B and κ are altered. We note the dependence of the solutions upon the magnitude of both the elastic control parameter κ and the compression control parameter B. It is clear from the figure that when κ is large, that is when $K_1^a > K_1^n$, the layer normal does not tend to reorient towards the director. It only starts to reorient towards the equilibrium state $\vartheta = 0$ once the director angle ζ has dropped to $\zeta \approx \vartheta_0$. When κ is small, i.e. when $K_1^a < K_1^n$, the layer normal increases to align with the director before decreasing again towards $\vartheta = 0$. Again, this is physically understandable since large κ mean that the layers are less likely to

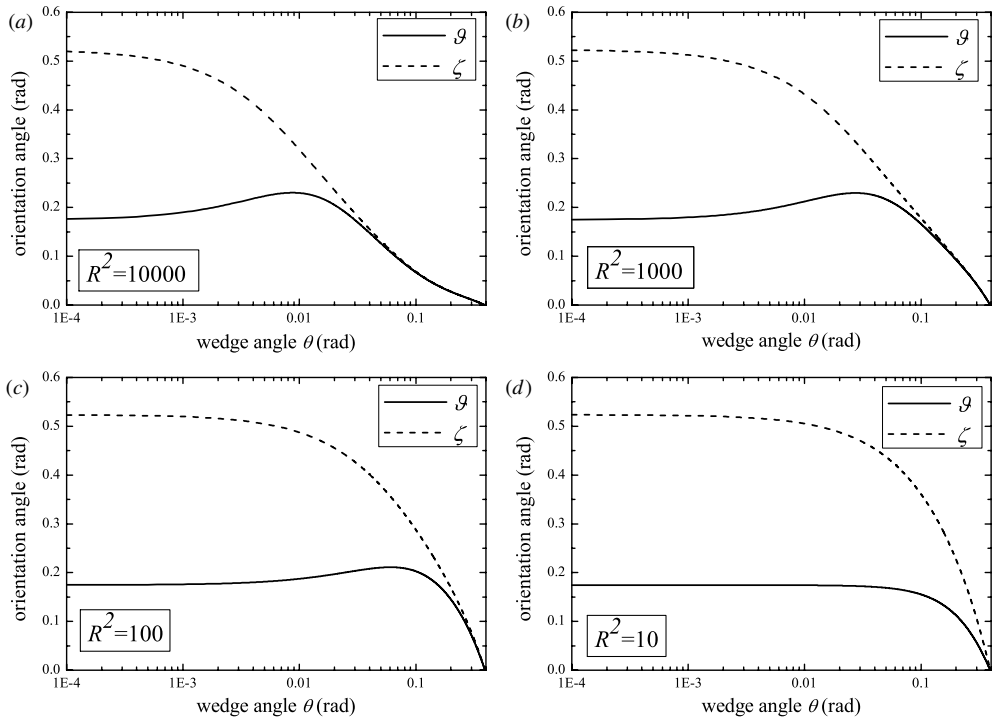

Figure 12. Solutions for $\vartheta(\theta)$ (solid lines) and $\zeta(\theta)$ (dashed lines) for the indicated values of the radius $\bar{R}$ of the layers being studied. The remaining parameters have been set as $\alpha = \pi/4$, $\zeta_0 = \pi/6$, $\vartheta_0 = \pi/18$, $B = 1$ and $\kappa = 1$. Discussion of observations can be found in the main text.

reorient than the director. We also note the dependence on the control parameter B: when B is large, that is when $B_0 > B_1$, we find that the director orients towards the layer normal closer to the boundary than it does when $B = 1$. This is physically understandable since if the layers have a larger molecular compression then the director would be expected to attempt to realign over a shorter distance.

4. Compression and coupling at large R

We now consider the case where the bulk free energy is of the form

$$w_B = \tfrac{1}{2}B_0(|\nabla\Phi| + \mathbf{a}\cdot\mathbf{n} - 2)^2 + \tfrac{1}{2}B_1(1 - (\mathbf{n}\cdot\mathbf{a})^2), \tag{4.1}$$

where B_0 and B_1 are defined earlier. This will allow us to determine the relative importance and interplay between compression and coupling and can be viewed as looking at the sample at very large R where the splay energies will be minimized. We again consider the two cylindrical set-ups described in figure 1, without imposing director and layer tilt on any boundaries. This new energy shall be minimized as before, and the resulting equations studied. We find, in both cases, that the Euler–Lagrange equations result in one nonlinear equation in two unknowns, the angles describing the orientation of the director and the layer normal. Bounds for the director are then found via this governing equation. The analysis in this section is considered in a more substantial context when a form for the layer function Φ is not imposed [20].

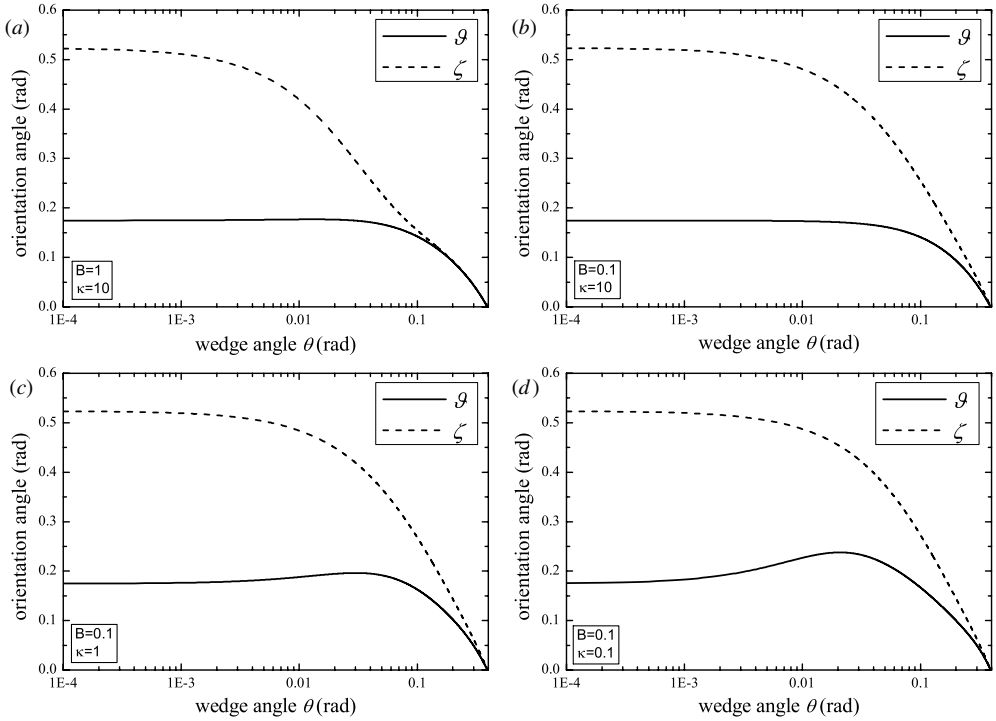

Figure 13. Solutions for $\zeta(\theta)$ (dashed lines) and $\vartheta(\theta)$ (solid lines) for the layers of radius around $\bar{R}^2 = 1000$ and indicated values of the control parameters B and κ. The remaining parameters have been set as $\alpha = \pi/4$, $\zeta_0 = \pi/6$ and $\vartheta_0 = \pi/18$. Discussion of observations can be found in the main text.

We consider first the geometrical set-up described in figure 1(*a*), without the imposed boundaries or director and layer normal tilt, i.e. we assume the layer normal, layer function and director are given via the relations (2.11), (2.16) and (3.1). The energy density function can then be written as

$$w_B = \tfrac{1}{2}B_0(\sec\delta + \cos(\delta - \zeta) - 2)^2 + \tfrac{1}{2}B_1 \sin^2(\delta - \zeta), \tag{4.2}$$

where we assume $\delta = \delta(z)$ and $\zeta = \zeta(z)$ as before. Employing the Euler–Lagrange equations results in the governing equation

$$B_0(\sec\delta + \cos(\delta - \zeta) - 2)\sec\delta\tan\delta = 0, \tag{4.3}$$

given that $\delta(z_0) = 0$. It is clear that the trivial solution $\delta \equiv \zeta \equiv 0$ exists. However, we can also find bounds on the angle δ which defines the orientation of the layer normal. Since B_0 is a nonzero constant, and assuming that $\delta \neq \zeta \neq 0$, equation (4.3) provides us with the condition

$$\zeta = \delta - \cos^{-1}(2 - \sec\delta). \tag{4.4}$$

Hence, for ζ to be a real angle we are forced into the constraint $-\sec^{-1} 3 \leqslant \delta \leqslant \sec^{-1} 3$. Of course, values of δ which satisfy this constraint could possibly provide ζ such that $\zeta < -\pi/2$ or $\zeta > \pi/2$ which would not make physical sense. If we consider ζ such that $-\pi/2 < \zeta < \pi/2$ then δ must also satisfy the relation $-\pi/2 < \delta - \cos^{-1}(2 - \sec\delta) < \pi/2$. Numerical calculations show that δ must lie within the range $-\pi/4 \lesssim \delta \lesssim \pi/3$, giving ζ in the range $-\pi/2 \lesssim \zeta \lesssim 0$.

If we consider the geometrical set-up described in figure 1(*b*), without the imposed boundaries or director and layer normal tilt, i.e. with layer normal, layer function and director are given via the relations (2.13), (2.15) and (3.17). The energy density function can then be written as

$$w_B = \frac{1}{2}B_0\left(\sec\vartheta\exp\int_{\theta_0}^{\theta}\tan\vartheta(t)\,\mathrm{d}t + \cos(\vartheta-\zeta) - 2\right)^2 + \frac{1}{2}B_1\sin^2(\vartheta-\zeta), \tag{4.5}$$

where we assume $\vartheta = \vartheta(\theta)$ and $\zeta = \zeta(\theta)$ as before. Minimization of this free energy results in the governing equation

$$2B_0\left(\sec\vartheta\exp\int_{\theta_0}^{\theta}\tan\vartheta(t)\,\mathrm{d}t + \cos(\vartheta-\zeta) - 2\right)\sec\vartheta\tan\vartheta\exp\int_{\theta_0}^{\theta}\tan\vartheta(t)\,\mathrm{d}t = 0, \tag{4.6}$$

given that $\vartheta(\theta_0) = 0$. Neglecting the trivial solution $\vartheta \equiv 0$ results in a condition analogous to (4.4), and the statements which follow it can be repeated here.

5. Conclusions and discussion

In this paper, we have identified a technique for finding nonlinear forms of the layer function Φ for smectic A liquid crystals in several geometrical set-ups. The general technique involves assuming a form for the layer normal **a**, which is seen from geometrical considerations, and then using the relation $\mathbf{a} = \nabla\Phi/|\nabla\Phi|$ to construct a partial differential equation, or system of equations, for Φ. In some circumstances, e.g. when the angle which defines the layer normal is assumed to be dependent on only one variable (as seen in the experimental work by Elston [8]), the partial differential equation can be solved using the method of characteristics to find a nonlinear form for the layer function. This is of extreme importance as until now, many have assumed a linear form.

A form for the free energy density of a smectic A liquid crystal with variable layers has been taken from the literature [19] and used to construct the free energy for two situations of cylindrically layered smectic A, when the layer normal is dependent on z and when the layer normal is dependent on θ. The Euler–Lagrange equations for both scenarios are constructed and studied. The problem considered where the layer normal is dependent on z is compared with a planar-layered scenario studied previously [18].

When the layer normal is assumed to have dependence in the z-direction only, the Euler–Lagrange equations are solved numerically, and compared to their planar-layered counterparts in [18]. We see that for layers of large radius, i.e. when the cylindrical layers are locally planar, the previous results of Stewart [18] are obtained. However, when a layer of finite radius are studied, we see that the angles which determine the layer normal and the director do not collapse to zero in the bulk. Instead, they remain mostly nonzero, but practically constant, throughout the bulk. The boundary layer phenomena are also studied, we find that the layer normal and the director are sensitive to changes in the radius and the control parameters κ and B. Using the numerical data from the solution of the Euler–Lagrange equations, we also calculate the integrated angle of inclination across the domain wall as a function of the radius of the layers. We find that it can be approximated by a simple ratio of powers. Dependence of the angles on the boundary conditions are also studied. We see that the angles always realign around $z = O(1) - O(10)$, apart from one case; when $\delta_0 = \zeta_0 = 0$ both angles remain fixed on their boundary values throughout the full sample, as expected.

When the liquid crystal is confined to have smectic layers in a wedge of angle α (which was not varied), and the layer normal is assumed to have dependence in the θ-direction only, the Euler–Lagrange equations are studied. In a similar manner to the previous scenario, the

Euler–Lagrange equations are solved numerically and the results studied. We find once more that the layer normal and the director and sensitive to changes in the radius and the two control parameters κ and B. We find that the angles defining the director and the layer normal change greatly as we study layers of variable radius. This suggests that for cylindrical samples of liquid crystals, the layer normal and the director are functions of at least two variables, that is, a variable which changes within the layers and one which crosses the smectic layers. Therefore the assumption made by Stewart [18] for planar-layered smectic A, that the layer normal and director should only be dependent on the variable which changes within the layers, should not be used for cylindrically layered smectic A, unless only individual layers are to be studied. If this assumption is not made for cylindrical samples then the method detailed in this paper will not result in a nonlinear form of the smectic layer function, but an unsolvable partial differential equation for it. Nevertheless, in making this assumption, we have managed to construct, and solve, Euler–Lagrange equations for two situations and show the dependence of the radius and the material parameters on the realignment of the layer normal and the director.

It can be seen in both theoretical experiments that there are apparent dependencies on the radius. Some surprising results are made in the limiting case $\bar{R} \to 0$. It may be the case that for small $\bar{R}$ the dynamic theory of Stewart [19] will not hold. This may be physically relevant as it is doubtful that cylindrical layers of such small radius could exist in experimental situations, and the liquid crystal may become an isotropic fluid in the centre of the sample. It may be intuitive to define a minimum allowed radius for the formation of smectic layers as considered in [22].

If the angles which define the director and layer normal are assumed to also have dependence on two spatial variables then the forms discussed for the layer function in the main body of the text may not be assumed. However, it is possible to construct a third Euler–Lagrange equation, for the variations in Φ (which would then be a function of three spatial variables), and solve numerically. Much added information on the form of the layer function can be found [20] which will fuel debate on the form of the free energy density used here.

The case where the splay energy contributions to the bulk free energy are negligible is also discussed briefly. This is physically relevant for layers of such large radius where the splay energies are negligible in comparison to the compressional energy B_0 and the coupling energy B_1, which are assumed to be roughly of the same order. We find, by minimizing the Euler–Lagrange equations, bounds for the angles which define the orientation of the layer normal and the director in the two cylindrical geometries studied. This analysis can be extended for when a form for the layer function has not been assumed, that is, when the layer normal is assumed to be a function of two spatial variables [20].

As mentioned previously, the elementary form for the free energy density used here was taken from formulations elsewhere in the literature [18, 19]. However, it could possibly be seen that this free energy is an elementary nonlinear construction of what may be a more intricate nonlinear form. It is hoped that in the near future a more expansive fully nonlinear free energy density could be constructed in order to test the nonlinear forms of the smectic layer function contained in this paper and further work on the layer function Φ [20].

Finally, we have assumed in this paper that it is possible to set boundary conditions which determine the form of the smectic layers, just as we can determine the form of the director on the boundary. This cannot be achieved experimentally. However, this work could be extended in a manner similar to the paper by De Vita and Stewart [6] where they determine equilibrium configurations for planar-layered smectic A under strong and weak anchoring conditions for the director and introduce conventional natural boundary conditions on the smectic layer tilt rather than impose a prescribed layer tilt. The paper by De Vita and Stewart is a natural progression of the paper by Stewart [18] (which invokes prescribed boundary conditions for

the layer normal) and can therefore be utilized to progress the ideas contained within this paper to solve for Euler–Lagrange equations without a forced layer tilt on the boundaries.

References

[1] Atkinson K and Han W 2003 *Elementary Numerical Analysis* (New York: Wiley)
[2] Auernhammer G K, Brand H R and Pleiner H 2000 The undulation instability in layered systems under shear flow—a simple model *Rheol. Acta* **39** 215–22
[3] Auernhammer G K, Brand H R and Pleiner H 2002 Shear-induced instabilities in layered liquids *Phys. Rev.* E **66**
[4] Auernhammer G K, Brand H R and Pleiner H 2005 Shear-induced instabilities in layered liquids *Phys. Rev.* E **71** (erratum)
[5] de Gennes P G and Prost J 1993 *The Physics of Liquid Crystals* 2nd edn (Oxford: Oxford University Press)
[6] De Vita R and Stewart I W 2008 Influence of weak anchoring upon the alignment of smectic A liquid crystals with surface pretilt *J. Phys.: Condens. Matter* **20** 335101
[7] E W 1997 Nonlinear continuum theory of smectic-A liquid crystals *Arch. Rat. Mech. Anal.* **137** 159–75
[8] Elston S J 1994 The alignment of a liquid crystal in the smectic A phase in a high surface tilt cell *Liq. Cryst.* **16** 151–7
[9] Garabedian P R 1964 *Partial Differential Equations* (New York: Wiley)
[10] Kléman M and Parodi O 1975 Covariant elasticity for smectics A *J. Phys.* **36** 671–81
[11] Maplesoft *Maple 8* (Waterloo, Canada)
[12] OriginLab Corp. *Origin 8* (Northampton, MA)
[13] Ribotta R and Durand G 1977 Mechanical instabilities of smectic-A liquid crystals under dilative or compressive stresses *J. Phys.* **38** 179–204
[14] Soddemann T, Auernhammer G K, Guo H, Dünweg B and Kremer K 2004 Shear-induced undulation of smectic-A: molecular dynamics simulations vs. analytical theory *Eur. Phys. J.* E **13** 141–51
[15] Stewart F and Stewart I W 2007 A novel method for measuring compression constants in smectics *Mol. Cryst. Liq. Cryst.* **478** 779–88
[16] Stewart I W 2003 Layer distortions induced by a magnetic field in planar samples of smectic C liquid crystals *Liq. Cryst.* **30** 909–20
[17] Stewart I W 2004 *The Static and Dynamic Continuum Theory of Liquid Crystals* (London: Taylor and Francis)
[18] Stewart I W 2007 The alignment of smectic A liquid crystals with director tilt on the boundaries *J. Phys. A: Math. Theor.* **40** 5297–318
[19] Stewart I W 2007 Dynamic theory for smectic A liquid crystals *Contin. Mech. Thermodyn.* **18** 343–60
[20] Walker A J unpublished details
[21] Walker A J 2008 Theoretical studies of smectic liquid crystals subjected to flow, perturbations, magnetic fields and various applied boundary conditions *PhD Thesis* University of Strathclyde
[22] Walker A J and Stewart I W 2007 Periodic disturbances in cylindrically layered smectic A *Mol. Cryst. Liq. Cryst.* **478** 788–99